The $d_{x^2-y^2}$-wave superconducting gap in $Bi_2Sr_2CaCu_2O_8$: scanning tunnelling microscope spectroscopy

The $d_{x^2-y^2}$-wave superconducting gap in $Bi_2Sr_2CaCu_2O_8$: scanning tunnelling microscope spectroscopy

Koji Suzuki†, Koichi Ichimura†, Kazushige Nomura† and Shunji Takekawa‡

† Division of Physics, Hokkaido University, Sapporo 060-0810, Japan
‡ National Institute for Research in Inorganic Materials, Tsukuba, Ibaraki 305-0044, Japan

Abstract. We have carried out electron tunnelling spectroscopy on $Bi_2Sr_2CaCu_2O_8$ single crystals with the use of a scanning tunnelling microscope at 4.2 K. A conductance peak structure was observed near zero bias voltage for the tunnelling along the Cu–O bonding direction. A clear superconducting gap was observed for the tunnelling along the Cu–Cu direction. Curves along the Cu–O and Cu–Cu directions are consistent with the $d_{x^2-y^2}$-wave pairing symmetry which has line-nodes along the Cu–Cu direction, taking into account the periodic arrangement of surface oxygen atoms.

Since the discovery of high-T_c cuprates, many investigations have been carried out with the aim of establishing the symmetry of the superconducting pair wave function, which is a very important clue to the mechanism of the superconductivity. The symmetry of the pair wave function is reflected in the electronic density of states near the Fermi level in the superconducting phase. Scanning tunnelling microscope (STM) spectroscopy is a powerful method which can be used to observe the electronic density of states directly with high resolution in energy. In STM spectroscopy measurement at the cleaved Bi–O surface of $Bi_2Sr_2CaCu_2O_8$ single crystals, a clear superconducting gap structure was observed [1–4]. These results suggest that the superconducting gap is anisotropic. Some groups carried out STM spectroscopy measurements with tunnelling in the a–b plane of high-T_c superconductors, where the anisotropy of the superconducting gap is expected to be observed [4–8]. Kashiwaya *et al* [5] reported first the anomaly near zero bias voltage, which is the so-called zero-bias conductance peak (ZBCP) structure [9–11], for highly (100)-oriented $YBa_2Cu_3O_{7-\delta}$ thin films. However, they recently reported that the ZBCP is observed mainly for highly (110)-oriented thin films [6]. Tanaka *et al* [7] observed the ZBCP structure and the superconducting gap structure along the [100] and [110] directions, respectively, in $La_{2-x}Sr_xCuO_4$ ($x = 0.10$, 0.15) single crystals. Although these results suggest that the superconducting gap is anisotropic in the a–b plane, the results have not converged yet. Therefore, it is important to clarify the functional form of the a–b-plane anisotropy. With this viewpoint, we have observed tunnelling spectra for varying tunnelling direction in the a–b plane of $Bi_2Sr_2CaCu_2O_8$ single crystals. Conductance curves observed along directions intermediate between [100] (the Cu–O bonding direction) and [110] (the Cu–Cu bonding direction) were discussed in our previous paper [12], where we explained those curves in terms of a $d_{x^2-y^2}$-wave gap. In this article, we report tunnelling spectra observed along the [100] and [110] directions and discuss the symmetry of the pair wave function in the superconducting phase.

The $Bi_2Sr_2CaCu_2O_8$ single crystals used in this study were grown by the floating-zone method. The superconducting transition temperature T_c was determined as $T_c = 87$ K from the mid-point of the resistive transition. As-grown single crystals are plate-like along the *a–b* plane. The samples used in this study typically had dimensions of 1 mm $\times$ 1 mm $\times$ 0.05 mm. The crystal orientation was determined by x-ray diffraction, and it was ensured that these single crystals grew along the [110] direction. Clean lateral surfaces perpendicular to the [100] and [110] directions were prepared by cutting them with a razor-blade at room temperature. The cutting was carried out in air, because we know from experience that the surface of a $Bi_2Sr_2CaCu_2O_8$ single crystal is very stable [4, 12, 13]. We ensured that each cut surface was flat with an optical microscope. Furthermore, we observed a typical cut surface with a scanning electron microscope (SEM) and checked its flatness. The cut samples were immediately set into the STM probe cell [13]. The STM probe cell was filled with thermal exchange helium gas to achieve a thermal equilibrium state. A mechanically sharpened Pt–Ir alloy wire was used as the STM tip. Tunnelling differential conductance curves were observed in the vacuum tunnelling configuration where the STM tip does not contact the sample surface. Tunnelling differential conductance curves were observed directly by the lock-in technique with a 1 kHz ac modulation of 1 mV superposed on the bias voltage. In this study, the bias voltage is applied to the STM tip. Hence the conductance at positive bias corresponds to the density of states below the Fermi level.

Figure 1(a) shows tunnelling differential conductance curves observed at 4.2 K along the [100] direction with varying tip position. These curves were observed for initial tunnelling current $I_0 = 15$ nA for the bias voltage $V_0 = 100$ mV, where I_0 is reduced exponentially with increasing distance between the tip and the sample surface. Positions A, B, C, D and E were aligned at intervals of about 10 nm on the cut surface. The observed curves do not show the superconducting gap structure, in which the differential conductance is reduced near zero bias voltage. Moreover, a large differential conductance remains near zero bias voltage for these curves. The shape of the observed curves depends on the tip position. In the curves taken at positions A and C, a sharp peak structure was observed near zero bias voltage. This corresponds to the so-called ZBCP structure [9–11]. At positions B, D and E, the conductance near zero bias voltage is as large as that of the normal state. There is a possibility that such tip position dependence of ZBCP is due to inhomogeneity of the cut surface. However, such clear tip position dependence was not observed along intermediate directions between [100] and [110], where essentially the same superconducting gap structure was observed irrespective of the tip position [12]. The cause of this tip position dependence is probably the local disorder of the arrangement of surface oxygen atoms as described below. The differential conductance increases with the bias voltage in the high-bias-voltage region, as has been reported frequently [2–4]. It is deduced that such an energy dependence of the background conductance is brought about by the energy dependence of the tunnelling matrix element, which is due to the complex structure of the tunnelling barrier [13]. Figure 1(b) shows tunnelling differential conductance curves observed for a different area, which is separated by several hundreds of micrometres from the area for which the tunnelling spectra shown in figure 1(a) were obtained. Positions A–I were aligned at intervals of about 10 nm. Essentially the same ZBCP structure was observed irrespective of the tip position, in contrast to the case shown in figure 1(a). The peak is broader than that in figure 1(a). This is probably caused by the lifetime broadening of the one-electron level. The behaviour in the high-bias-voltage region is flat. This means that the tunnelling matrix element is almost constant over the whole voltage region. Its energy dependence is probably modified by the surface conditions. If the sample surface has less disorder, the tunnelling matrix element is expected to be independent of the energy.

As shown in figure 2, the detailed shape of this ZBCP depends on the distance of the tip
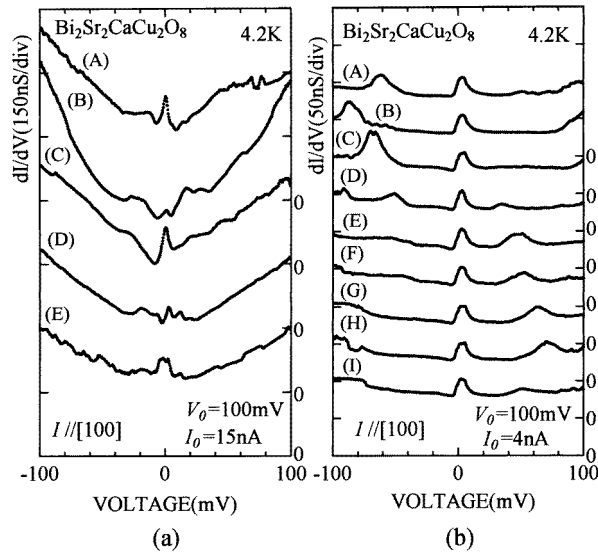
Figure 1. Tunnelling differential conductance curves observed at 4.2 K along the [100] direction with varying tip position. The curves in (a) and (b) were observed for different areas, which are separated by several hundreds of micrometres on the cut surface. These curves were observed for $I_0 = 15$ nA (a) and 4 nA (b) for $V_0 = 100$ mV, respectively. In each figure, the positions were aligned at intervals of about 10 nm in each area on the cut surface, and the zero-conductance line of each curve is shifted by one division for clarity.
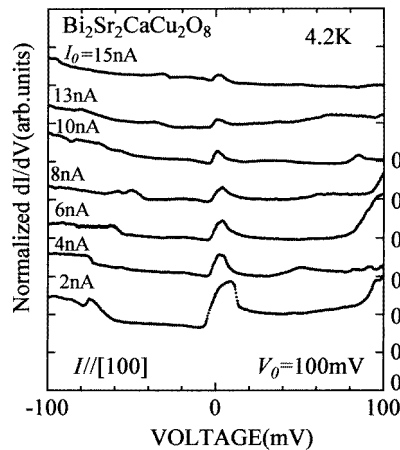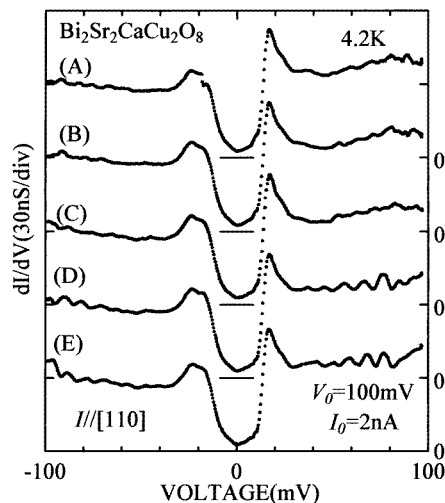

Figure 2. Tunnelling differential conductance curves observed along the [100] direction at 4.2 K with varying tip distance. These curves were observed for $I_0 = 2, 4, 6, 8, 10, 13$ and 15 nA for $V_0 = 100$ mV. Each curve is normalized at $V = 30$ mV, and the zero-conductance line of each curve is shifted by one division for clarity.

from the sample surface. These curves were observed at the position I in figure 1(b). The peak height is reduced with decreasing tip distance. This tip distance dependence was found reproducibly at fixed positions. There is a possibility that this tip distance dependence is due to the modification of the k-dependence of the tunnelling transition probability [12, 14]. An

electron whose kinetic energy component perpendicular to the tunnelling barrier is large has a large probability of tunnelling. This k-dependence is governed by the tip distance. As the tip distance becomes large, the tunnelling transition probability begins to depend strongly on the wave vector k. Accordingly, the peak height is expected to reduce with decreasing tip distance. However, as described below, the k-dependence of the tunnelling is determined mainly by Bloch's electron wave function for high-T_c cuprates. We do not yet have a concrete model for explaining this tip distance dependence in such a case. Nevertheless, it is likely that the modification of the k-dependence of the tunnelling probability should also be taken into account for a quantitative explanation.

This ZBCP structure was also observed for another sample along the [100] direction, and essentially the same tip distance dependence was observed. The clear superconducting gap structure was never observed along the [100] direction in our study.

Figure 3 shows tunnelling differential conductance observed at 4.2 K along the [110] direction with varying tip position. These curves were observed for $I_0 = 2$ nA and $V_0 = 100$ mV. Positions A–E are aligned at intervals of about 10 nm on the cut surface. Essentially the same curve was observed irrespective of the tip position. These curves show a clear superconducting gap structure. The superconducting gap edge is clearly observed as an enhancement of the conductance at $V = 17$ mV. The value of $\Delta_{p-p} = 17$ meV, where the gap width is defined as $2\Delta_{p-p}$, is slightly smaller than the value of 25–40 meV obtained at the cleaved Bi–O surface [4]. The conductance is reduced to almost zero near zero bias voltage. The behaviour away from the gap edge is almost flat, as expected for the electronic density of states in the normal phase. We reported a similar result previously [4], where a clear superconducting gap structure with $\Delta_{p-p} = 25$ meV was observed along the [110] direction. The curves shown in figure 3 are asymmetric with respect to the Fermi level. The conductance at positive bias, which corresponds to the density of states below the Fermi level, is larger than that at negative bias. Similar results were reported by Renner and Fischer [1]. In our study, however, the observed curves are not always asymmetric with respect to the Fermi level [4, 12, 13], so we do not know whether this asymmetry is intrinsic or not. These curves


Figure 3. Tunnelling differential conductance curves observed at 4.2 K along the [110] direction with varying tip position. These curves were observed for $I_0 = 2$ nA for $V_0 = 100$ mV. Positions A, B, C, D and E were aligned at intervals of about 10 nm on the cut surface.

observed along the [110] direction are clearly different from those along the [100] direction. This means that the superconducting gap is highly anisotropic in the *a–b* plane.

It is claimed that the bound state is formed by the tunnelling around line-nodes on the Fermi surface of the d-wave superconducting gap, where the sign of the order parameter reverses [9–11]. According to the theory, the ZBCP structure is observed if the tunnelling occurs around the line-nodes. The ZBCP structure or no gap along the [100] direction may have other explanations such as contamination of the surface or disorder of the surface caused by cutting. In our study, however, the ZBCP is not observed along the *c*-axis and the directions intermediate between the [100] and [110] directions [4, 12, 13]. If the ZBCP were due to the destruction of the superconducting state at the cut surface, it would be observed also along these directions, especially along the intermediate directions where the cut surface was prepared by the same method. Therefore, the ZBCP structure observed along the [100] direction is most probably due to the line-nodes on the Fermi surface of the d-wave gap. In addition, the ZBCP is not explained by the anisotropic s-wave superconducting gap whose $\Delta(\mathbf{k})$ does not change in sign [9–11]. At first sight, our results for the [110] and [100] directions seem to suggest that the gap has d_{xy}-wave symmetry with line-nodes along the [100] direction. This symmetry is inconsistent with the result for directions intermediate between [100] and [110], where the observed curves are explained by the $d_{x^2-y^2}$-wave gap [12]. However, Tanaka *et al* [7] suggested that the electron tunnelling is determined by Bloch's electron wave function in the periodic arrangement of surface oxygen atoms in high-T_c cuprates. According to their theory, the tunnelling differential conductance curve is given as

$$\frac{\mathrm{d}I}{\mathrm{d}V}(V, r_t) \propto \int_0^{2\pi} \int_{-\infty}^{\infty} |\Psi_k(r_t)|^2 \frac{E - \mathrm{i}\Gamma}{\sqrt{(E - \mathrm{i}\Gamma)^2 - \Delta^2(\theta)}} \left\{ -\frac{\partial f(E + eV)}{\partial V} \right\} \mathrm{d}E \, \mathrm{d}\theta \qquad (1)$$

where θ is the angle from the [100] direction in the *a–b* plane, and $\Psi_k(r_t)$ is the tight-binding Bloch electron wave function with the wave vector $\mathbf{k}$ at the tip position r_t, where $\mathbf{k}$ is defined on the Fermi surface and is represented by θ. The effect of thermal broadening is introduced by the Fermi distribution function $f(E)$, and the parameter Γ represents the lifetime broadening of the one-electron level. The factor $|\Psi_k(r_t)|^2$ is calculated for the anti-bonding band formed by the Cu $3d_{x^2-y^2}$ orbital and the O $2p_\sigma$ orbital in the Cu–O plane, and this factor gives the $\mathbf{k}$-dependence to the tunnelling matrix element. We calculate $|\Psi_k(r_t)|^2$ for the [100] and [110] directions with their model, assuming a half-filled Fermi surface in the two-dimensional square lattice. Figure 4(a) shows a typical $|\Psi_k(r_t)|^2$ calculated for the [110] direction. The calculated $|\Psi_k(r_t)|^2$ has a small or zero value for the wave vector $\mathbf{k}$ around the [110] direction and has a large value for $\mathbf{k}$ around the [100] or [010] direction. Essentially the same result is obtained irrespective of the tip position. This means that the tunnelling occurs mainly via the electrons with wave vector $\mathbf{k}$ around the [100] or [010] direction rather than


(a) (b)
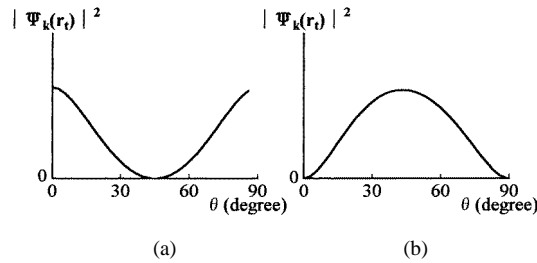
Figure 4. Typical functions $|\Psi_k(r_t)|^2$ calculated for the [110] direction (a) and the [100] direction (b). The [100] and [110] directions show exchanged behaviour.

the [110] direction. Figure 4(b) shows a typical $|\Psi_k(r_t)|^2$ calculated for the [100] direction. The calculated $|\Psi_k(r_t)|^2$ has a small or zero value for the wave vector k around the [100] direction and has a large value for k around the [110] direction. Essentially the same result is obtained irrespective of the tip position. This means that the main contribution to the tunnelling current is given by the electrons with wave vector k around the [110] direction rather than the [100] direction. Such tunnelling along the [100] and [110] directions is brought about by the interference effect of atomic orbitals on surface oxygen atoms. These calculation results are essentially the same as those given by Tanaka *et al* [7].

It is claimed that the anisotropy of the band dispersion should also be taken into account for high-T_c cuprates [3, 12]. According to the tight-binding approximation for the two-dimensional square lattice, the anisotropy of the band dispersion, $N(\theta) = 1/|\nabla_k \varepsilon(k)|$, has large and small values around the [100] and [110] directions, respectively [3, 12]. This factor also acts as a weight factor, like $|\Psi_k(r_t)|^2$. However, the in-plane angular dependence of the differential conductance is determined by $|\Psi_k(r_t)|^2$ mainly. The anisotropy of the band dispersion is rather less important [12].

As is known from the above discussion, exchanged behaviour of the [110] and [100] directions probably occurs in STM spectroscopy for high-T_c cuprates. One expects for the $d_{x^2-y^2}$-wave symmetry gap the ZBCP to be observed for tunnelling along the [100] direction and a clear gap structure to be present along the [110] direction. This means that our results for the [100] and [110] directions are consistent with the $d_{x^2-y^2}$-wave gap qualitatively. Figure 5 shows the fitting of the curve observed along the [110] direction, which is shown as curve C in figure 3, to the $d_{x^2-y^2}$-wave gap model $\Delta = \Delta_0 \cos 2\theta$. In this fitting, we fitted the functional form in the low-bias-voltage region [4]. We assumed that the tunnelling matrix element is proportional to $|\Psi_k(r_t)|^2$, shown in figure 4(a). The calculated curve, shown as the broken curve, reproduces the observed superconducting gap structure near zero bias voltage with the lifetime broadening of the one-electron level. It needs a more concrete model to explain how the bound state is formed by the tunnelling along the [100] direction for the $d_{x^2-y^2}$-wave gap. However, according to this theory, the ZBCP is most probably observed along the [100]
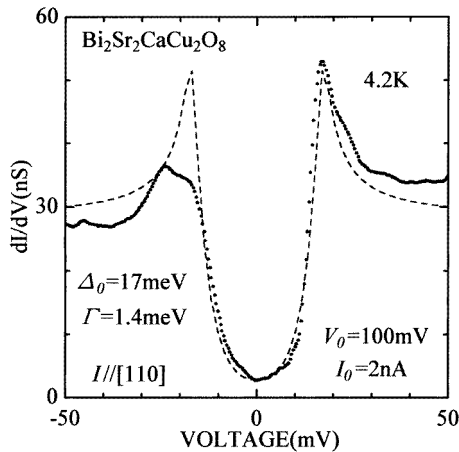
Figure 5. Fitting of the curve observed along the [110] direction, which is shown as curve C in figure 3, to the $d_{x^2-y^2}$-wave gap model. The calculated $|\Psi_k(r_t)|^2$ shown in figure 4(a) was used in this fitting. The broken curve represents the calculated conductance curve, taking into account the broadening of the one-electron level $\Gamma = 1.4$ meV.

direction. As for the tip position dependence of ZBCP shown in figure 1(a), the local disorder of the arrangement of surface oxygen atoms is likely to play an important role, and it is deduced that the arrangement has less disorder in the case of figure 1(b).

Our result is analogous with the result for $La_{2-x}Sr_xCuO_4$ ($x = 0.10, 0.15$) single crystals given by Tanaka *et al* [7]. However, Alff *et al* [6] observed the ZBCP along the [110] direction frequently in measurements on highly oriented $YBa_2Cu_3O_{7-\delta}$ thin films. We do not know the cause of this difference yet. However, we think that the ZBCP structure observed along the [100] direction is crucial.

A surface perpendicular to a direction intermediate between [110] and [100] has essentially poor periodicity of surface oxygen atoms. The period of the atomic arrangement is fairly large as compared with the ionic radius of O^{2-} in these directions, and the interference effect due to the periodic arrangement of surface oxygen atoms can hardly arise. Therefore, the local electronic state contributes to the differential conductance curves in these directions. We explained curves observed along the directions intermediate between [110] and [100] in terms of a $d_{x^2-y^2}$-wave gap from such a point of view in our previous paper [12]. The curves observed along the [100] and [110] directions in this study are not decisive evidence of a $d_{x^2-y^2}$-wave gap. However, we conclude that the $d_{x^2-y^2}$-wave gap is formed in the superconducting phase of $Bi_2Sr_2CaCu_2O_8$ from the total a–b-plane angular dependence of the tunnelling differential conductance curves, including the curves observed along the directions intermediate between [100] and [110] (reference [12]).

In conclusion, the ZBCP structure and a clear superconducting gap structure were observed along the [100] and [110] directions, respectively. These curves are consistent with the $d_{x^2-y^2}$-wave gap taking into account the periodic arrangement of surface oxygen atoms in the Cu–O plane.

Acknowledgments

References

[1] Renner Ch and Fischer Ø 1995 *Phys. Rev.* B **51** 9208–18
[2] Murakami H and Aoki R 1995 *J. Phys. Soc. Japan* **64** 1287–92
[3] Manabe C, Oda M and Ido M 1997 *J. Phys. Soc. Japan* **66** 1776–84
[4] Ichimura K, Suzuki K, Nomura K and Takekawa S 1995 *J. Phys.: Condens. Matter* **7** L545–51
[5] Kashiwaya S, Koyanagi M, Matsuda M and Kajimura K 1994 *Physica* B **194–196** 2119–20
[6] Alff L, Takashima H, Kashiwaya S, Terada N, Ihara H, Tanaka Y, Koyanagi M and Kajimura K 1997 *Phys. Rev.* B **55** 14 757–60
[7] Tanaka S, Ueda E, Sato M, Tamasaku K and Uchida S 1995 *J. Phys. Soc. Japan* **64** 1476–80
[8] Kane J and Ng K W 1996 *Phys. Rev.* B **53** 2819–26
[9] Hu C R 1994 *Phys. Rev. Lett.* **72** 1526–9
[10] Tanaka Y and Kashiwaya S 1995 *Phys. Rev. Lett.* **74** 3451–4
[11] Matsumoto M and Shiba H 1995 *J. Phys. Soc. Japan* **64** 1703–13
[12] Suzuki K, Ichimura K, Nomura K and Takekawa S 1999 *Phys. Rev. Lett.* submitted
[13] Ichimura K and Nomura K 1993 *J. Phys. Soc. Japan* **62** 3661–79
[14] Wolf E L 1989 *Principles of Electron Tunneling Spectroscopy* (New York: Oxford University Press) p 23